

The β_4 -Subunit of the Large-Conductance Potassium Ion Channel $K_{Ca}1.1$ Regulates Outflow Facility in Mice

Jacques A. Bertrand,¹ Martin Schicht,² W. Daniel Stamer,³ David Baker,⁴
Joseph M. Sherwood,¹ Elke Lütjen-Drecoll,² David L. Selwood,⁵ and Darryl R. Overby¹

¹Department of Bioengineering, Imperial College London, London, United Kingdom

²Department of Anatomy II, University of Erlangen-Nürnberg, Erlangen, Germany

³Department of Ophthalmology, Duke University, Durham, North Carolina, United States

⁴Department of Neuroinflammation, University College London Institute of Neurology, University College London, London, United Kingdom

⁵Department of Medicinal Chemistry, Wolfson Institute for Biomedical Research, University College London, London, United Kingdom

Correspondence: Darryl R. Overby, Department of Bioengineering, Imperial College London, London SW7 2AZ, United Kingdom; d.overby@imperial.ac.uk.

Received: August 20, 2019

Accepted: January 9, 2020

Published: March 23, 2020

Citation: Bertrand JA, Schicht M, Stamer WD, et al. The β_4 -subunit of the large-conductance potassium ion channel $K_{Ca}1.1$ regulates outflow facility in mice. *Invest Ophthalmol Vis Sci.* 2020;61(3):41. <https://doi.org/10.1167/iovs.61.3.41>

PURPOSE. The large-conductance calcium-activated potassium channel $K_{Ca}1.1$ (BK_{Ca} , maxi-K) influences aqueous humor outflow facility, but the contribution of auxiliary β -subunits to $K_{Ca}1.1$ activity in the outflow pathway is unknown.

METHODS. Using quantitative polymerase chain reaction, we measured expression of β -subunit genes in anterior segments of C57BL/6J mice (*Kcnmb1-4*) and in cultured human trabecular meshwork (TM) and Schlemm's canal (SC) cells (*KCNMB1-4*). We also measured expression of *Kcnma1/KCNMA1* that encodes the pore-forming α -subunit. Using confocal immunofluorescence, we visualized the distribution of β_4 in the conventional outflow pathway of mice. Using iPerfusion, we measured outflow facility in enucleated mouse eyes in response to 100 or 500 nM iberiotoxin (IbTX; $N = 9$) or 100 nM marventoxin (MarTX; $N = 12$). MarTX selectively blocks β_4 -containing $K_{Ca}1.1$ channels, whereas IbTX blocks $K_{Ca}1.1$ channels that lack β_4 .

RESULTS. *Kcnmb4* was the most highly expressed β -subunit in mouse conventional outflow tissues, expressed at a level comparable to *Kcnma1*. β_4 was present within the juxtacanalicular TM, appearing to label cellular processes connecting to SC cells. Accordingly, *KCNMB4* was the most highly expressed β -subunit in human TM cells, and the sole β -subunit in human SC cells. To dissect functional contribution, MarTX decreased outflow facility by 35% (27%, 42%; mean, 95% confidence interval) relative to vehicle-treated contralateral eyes, whereas IbTX reduced outflow facility by 16% (6%, 25%).

CONCLUSIONS. The β_4 -subunit regulates $K_{Ca}1.1$ activity in the conventional outflow pathway, significantly influencing outflow function. Targeting β_4 -containing $K_{Ca}1.1$ channels may be a promising approach to lower intraocular pressure to treat glaucoma.

Keywords: trabecular meshwork, outflow facility, ion channels, mechanotransduction, mouse models

Intraocular pressure (IOP) is determined by aqueous humor outflow facility. With decreasing facility, IOP becomes elevated, and elevated IOP is the major risk factor for glaucoma. The trabecular meshwork (TM) and inner wall endothelium of Schlemm's canal (SC) regulate outflow facility.^{1,2} Although the precise mechanism of facility regulation is not fully understood,³ volume, stiffness, and contractility of TM and SC cells are known to play important roles.⁴⁻⁸

The large-conductance calcium-activated potassium channel $K_{Ca}1.1$ (BK_{Ca} , maxi-K or Slo1) regulates cell volume and contractility in smooth muscle cells,⁹ as well as in TM and SC cells.^{5,10-12} The $K_{Ca}1.1$ channel opener, NS1619, increases outflow facility in porcine anterior segments.¹³ NS1619 also inhibits the decrease in outflow facility following perfusion with hypotonic saline in bovine anterior segments⁵ and, likewise, decreases TM cell volume¹³ and

smooth muscle cell contractility.¹⁴ Conversely, blocking $K_{Ca}1.1$ with iberiotoxin (IbTX) potentiates the facility decrease in response to hypotonic saline⁵ and inhibits the cell volume decrease in response to NS1619.¹³ IbTX also inhibits the facility increasing effect of nitric oxide donors in porcine anterior segments.¹⁵ $K_{Ca}1.1$ is thus involved in outflow facility regulation, apparently by regulating the volume or contractility of SC or TM cells.

$K_{Ca}1.1$ is composed of four α -subunits that form the potassium-selective transmembrane pore. Membrane depolarization or increased cytosolic calcium may activate $K_{Ca}1.1$, leading to channel opening, potassium efflux, and membrane depolarization.¹⁶ Association between α and auxiliary β -subunits, of which there are four types (β_{1-4}),¹⁷ regulates $K_{Ca}1.1$ sensitivity to voltage and calcium. β -subunits are differentially expressed in a tissue-specific



manner and affect the pharmacology of $K_{Ca}1.1$. For example, β_4 renders $K_{Ca}1.1$ relatively resistant to IbTX but sensitive to marrentoxin (MarTX), which has a smaller effect on $K_{Ca}1.1$ channels lacking β_4 .^{18–20}

In this study, we examine the expression of genes encoding the β -subunits of $K_{Ca}1.1$ in mouse anterior segments (*Kcnmb1-4*) and in human TM and SC cells (*KCNMB1-4*). We focus on β_4 , examining its localization in the TM and inner wall endothelium of SC. Using MarTX, we examine the influence of β_4 on outflow facility in enucleated mouse eyes. We also examine the effect of IbTX to investigate the influence of $K_{Ca}1.1$ channels that lack β_4 on outflow facility.

METHODS

Gene Expression

We used quantitative polymerase chain reaction (qPCR) to measure the expression of *Kcnma1* and *Kcnmb1-4* in mouse anterior eye segments and *KCNMA1* and *KCNMB1-4* in cultured human TM and SC cells. For mouse anterior segments, C57BL/6J mice ($N = 3$, 13-week-old males, Charles River UK Ltd., Margate, UK) were euthanized by cervical dislocation. Eyes were enucleated, trimmed of extraocular tissue, and hemisected at the equator. The lens was removed, and the anterior segments homogenized in TRIzol using a rotor-stator tissue homogenizer (Ultra-Turrax T10; VWR, Leicestershire, UK). Total RNA was extracted using PureLink RNA spin columns following manufacturer protocols (ThermoFisher Scientific, Waltham, MA, USA). RNA content was measured using a spectrophotometer (NanoDrop ND-1000; ThermoFisher Scientific), and 2 μ g of RNA was used to synthesize cDNA by reverse transcription (Superscript VILO; ThermoFisher Scientific). qPCR was carried out using TaqMan master mix and primers (see Supplementary Table S1). *GAPDH/Gapdh* was used as the reference gene. cDNA was analyzed in triplicate (QuantStudio 6 Flex; Applied Biosystems, ThermoFisher Scientific). Expression level relative to *GAPDH/Gapdh* was calculated using the Δ Ct method. Homogenized mouse brain tissue, which expresses *Kcnma1* and *Kcnmb4*,²¹ was used as a positive control. Mouse 3T3-L1 fibroblasts (passage 25), which do not express $K_{Ca}1.1$ channels,²² were used as a negative control. As the anterior segment contains various tissues, this approach was unable to attribute expression to TM or SC directly. Further, pooling tissues together may mask the actual gene expression within the TM or SC.

Human TM and SC cells were isolated and characterized from human donor eyes following established techniques.^{23–26} Cells were grown to confluency in T25 flasks and lysed using TRIzol. RNA extraction and quantification followed the methods described earlier for mouse anterior segments. These studies used TM cell strains TM86, TM93, and TM134 from donors aged 3 months, 35, and 51 years, respectively, and SC cell strains SC56 and SC67 from donors aged 29 and 44 years, respectively. TM and SC cells were used between passage 4 and 6. EA.hy926 human endothelial cells (ATCC CRL-2922; LGC standards, Middlesex, UK) were used at passage 8 as a positive control for *KCNMA1* and *KCNMB4* expression.²⁷

Microscopy

Whole globes from three adult mice (C57BL/6J) were fixed in 4% paraformaldehyde (Roth, Karlsruhe, Germany) for

4 hours and washed in PBS. The eyes were hemisected at the equator, and 10 μ m sagittal cryostat sections were cut. The sections were incubated in BLOTTO's Blocking Buffer (ThermoFisher Scientific) at room temperature for 1 hour to reduce nonspecific staining. Following three washes in Tris-buffered PBS, specimens were incubated with the primary antibody (Table 1) at 4°C overnight, washed three times with PBS, and incubated with a secondary antibody (goat anti-rabbit Alexa 488; Invitrogen A11070; 1:1000) for 75 minutes. For double immunolabeling, specimens were washed three times with PBS and incubated with the second primary antibody (Table 1) at 4°C overnight. After washing three times with PBS, sections were incubated with secondary antibody (goat anti-rat Cy3; Dianova, Dianova GmbH, Hamburg, Germany 112-169-003; 1:1000) for 1 hour. Sections were mounted on glass slides with a 1:1 mixture of PBS and glycerol containing DAPI to label cell nuclei (10 μ L of 2 mg/mL). The slides were examined with a Keyence Bioevo BZ9000 microscope (Keyence, Neu-Isenburg, Germany).

For electron microscopy, one MarTX perfused mouse eye (100 nM) and its paired contralateral vehicle perfused eye, were postfixed in OsO_4 and dehydrated. Whole eyes were embedded in Epon resin and 1 μ m semithin sagittal sections were cut using an ultramicrotome (Ultracut E; Reichert Jung, Vienna, Austria). Semithin sections were stained with toluidine blue and examined with a Keyence Bioevo BZ9000 microscope. Ultrathin sections through the TM were then cut, stained with uranyl acetate and lead citrate, and viewed with a transmission electron microscope (JEM 1400 plus; JEOL, MA, USA). Four regions were examined per eye.

Outflow Facility Measurements

We measured the effect of IbTX and MarTX on outflow facility in enucleated eyes from C57BL/6J mice (13-week-old males; Charles River UK Ltd., Margate, UK). We used a paired experimental design, in which one eye was perfused with IbTX or MarTX and the contralateral eye perfused with vehicle. We measured the relative difference in outflow facility between treated and untreated paired eyes. All procedures on living mice were carried out under the authority of a United Kingdom Home Office project license and adhered to the ARVO Statement for the Use of Animals in Ophthalmic and Vision Research.

IbTX was purchased from Tocris Bioscience (Abingdon, UK). MarTX was custom synthesized by Peptide Protein Research Limited (Fareham, UK) with the sequence FGLIDVKCFASSECWTACKKVTGSGQGKQNNQCRCY, as determined by Ji et al.²⁸ This sequence contains the N-terminal phenylalanine, which may be lacking from some commercial suppliers, but is critical for MarTX function.²⁹ MarTX was modified by the addition of propargyl (Pra) to the lysine at position 7 with the sequence FGLIDV[Pra]CFASSECWTACKKVTGSGQGKQNNQCRCY. Pra labeling was chosen because it is compatible with click-chemistry, and thereby allows fluorescent click labeling to localize MarTX in fixed specimens. Separate studies revealed successful MarTX labeling in fixed EA.hy926 cells, but labeling was undetectable within the mouse TM in situ (data not shown).

For perfusions, mice were humanely culled by cervical dislocation. Eyes were enucleated, affixed to a support platform using tissue glue, and submerged in PBS at 35°C. Using a micromanipulator and dissection microscope, the anterior

TABLE 1. Antibodies Used for Immunofluorescence Microscopy

Protein	Host Species	Company, Catalog Number	Dilution in PBS
Anti- $K_{Ca}1.1 \beta_4$	Rabbit	Alomone Labs; APC-061	1:50
PECAM-1/CD31	Rat	Biologend; 102401; Clone C390	1:50

TABLE 2. Expression of Genes Encoding the $K_{Ca}1.1$ Channel α -Subunit and the Four β -Subunits in Mouse Tissues ($N = 3$ mice) and Human Cells Measured by qPCR

	Gene Expression				
	<i>Kcnma1</i>	<i>Kcnmb1</i>	<i>Kcnmb2</i>	<i>Kcnmb3</i>	<i>Kcnmb4</i>
Mouse Tissue					
Brain	+	+	+	+/-	+
Anterior Segment	+	+	+/-	-	+
Human Cells					
	<i>KCNMA1</i>	<i>KCNMB1</i>	<i>KCNMB2</i>	<i>KCNMB3</i>	<i>KCNMB4</i>
Ea.Hy926	+	+/-	-	-	+
hSC58	+	-	-	-	+
hSC67	+	-	-	-	+
hTM93	+	+	+/-	-	+
hTM86	+	+/-	+/-	-	+
hTM134	+	+	+/-	-	+

Positive (+) indicates all samples tested gave Ct values lower than 35 cycles. Positive/negative (+/-) indicates that at least one sample tested gave a Ct value between 35 and 40 cycles. If all samples tested gave Ct values greater than 40 cycles, they were considered indistinguishable from background and marked negative (-). Full details of Ct values are available in Supplementary Figure S1.

chamber was cannulated within 10 to 15 minutes of death using a 33-gauge beveled metal needle (NanoFil, NF33BV-2; World Precision Instruments, Sarasota, FL, USA) connected to the iPerfusion system (Bioengineering Department, Imperial College London, UK).³⁰ The vehicle was Dulbecco's PBS containing divalent cations and 5.5 mM glucose (collectively referred to as DBG) that was passed through a 0.2- μ m filter prior to use. Paired eyes were perfused with either DBG or DBG containing IbTX or MarTX. We examined the effect of 100 nM IbTX ($N = 4$ pairs), 500 nM IbTX ($N = 5$), and 100 nM MarTX ($N = 12$).

IOP was set to 9 mm Hg for 1 hour to pressurize and acclimatize the eye to the perfusion environment. Flow into the eye was then measured over 7 increasing pressure steps from 6.5 to 16.5 mm Hg. The flow rate at each step was considered to have reached stability when the ratio of the flow rate to pressure changed by less than 0.1 nL/min/mm Hg per minute over a 5-minute window. Three pressure steps from three perfusions failed to reach stability and were excluded from further analysis. The stable flow rate Q and stable pressure P were calculated over the last 4 minutes of each step, and the $Q - P$ data were fit by a power-law relationship of the form

$$Q = C_r \left(\frac{P}{P_r} \right)^b P \quad (1)$$

The fitting yields C_r , which represents the value of outflow facility at a reference pressure P_r of 8 mm Hg, and b that characterizes the nonlinearity of the $Q-P$ relationship.³⁰ We then calculated the relative difference in C_r between treated and untreated contralateral eyes, defined as the ratio of C_r in the treated eye relative to that in the contralateral control eye minus unity. We tested whether the relative difference in facility was statistically different from zero using a weighted t -test on the log-transformed data, as previously described.³⁰ Facility values and relative changes in facility were then converted back into the linear domain

and reported in terms of the geometric mean and the 95% confidence interval on the mean.

RESULTS

Gene Expression

By qPCR, we detected positive expression ($Ct < 35$) of *Kcnma1*, *Kcnmb1*, and *Kcnmb4* in mouse anterior segments ($N = 3$; Table 2 and Supplementary Fig. S1A). *Kcnmb2* and *Kcnmb3* had Ct values higher than 35 and 40, respectively, and were thus considered low expression or below the limit of quantification. ΔCt values ($\Delta Ct = Ct[\text{gene}] - Ct[\text{Gapdh}]$) for *Kcnma1* and *Kcnmb4* were similar for mouse anterior segments (7.6 and 8.5, respectively), whereas ΔCt for *Kcnmb1* was greater (10.1), indicating roughly four-fold lower expression (Supplementary Fig. S1A). Homogenized mouse brain was positive for all genes except *Kcnmb3*, which was expressed at low levels. Mouse 3T3-L1 fibroblasts expressed low levels of *Kcnma1* and *Kcnmb4*. *Kcnmb1-3* were below the limit of quantification (40 cycles).

Human TM cells expressed *KCNMA1*, *KCNMB1*, and *KCNMB4*, but low levels of *KCNMB2* and undetectable levels of *KCNMB3* (Table 2 and Supplementary Fig. S1B). Human SC cells expressed *KCNMA1* and *KCNMB4*, but no other β -subunit genes (Table 2 and Supplementary Fig. S1B). β_4 was the most highly expressed β -subunit in TM cells, and the sole β -subunit in SC cells. EA.hy926 cells, used as a positive control, primarily expressed *KCNMA1* and *KCNMB4*. TM and SC cells express similar amounts of *KCNMA1* relative to EA.hy926 cells, but several-fold higher levels of *KCNMB4* (Supplementary Fig. S1B).

We then analyzed published microarray data (GEO ID: GSE32169) from primary human TM cells deposited by Porter et al.³¹ Consistent with our qPCR data described earlier, *KCNMB4* was the most highly expressed β -subunit gene, with expression levels comparable to *KCNMA1*. *KCNMB1* and *KCNMB3* were expressed at lower levels,

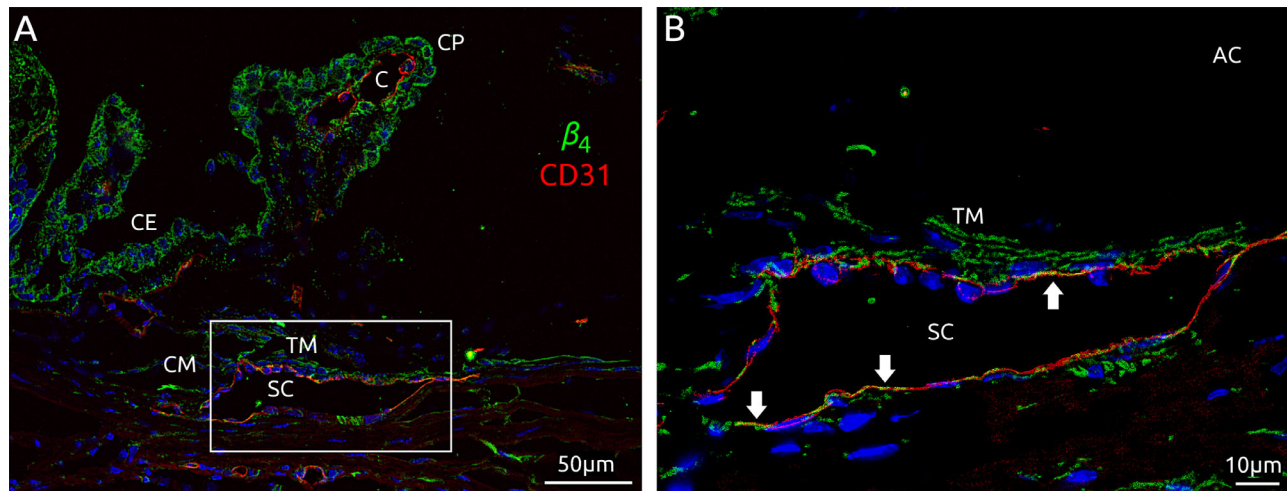


FIGURE 1. Localization of β_4 in the iridocorneal angle of the mouse eye. Boxed region in (A) is shown magnified in (B). Labeling of β_4 is shown in green, CD31 in red, and nuclei stained by DAPI in blue. AC, anterior chamber; CM, ciliary muscle; CP, ciliary process; CE, ciliary epithelium; C, ciliary process capillary. Arrows show areas of colocalization of β_4 with CD31 along the inner and outer walls of SC.

and *KCNMB2* was the lowest expressed (Supplementary Fig. S1C). These data show that β_4 is the most highly expressed auxiliary β -subunit of the $K_{Ca}1.1$ channel in mouse anterior segments, as well as in cultured human TM and SC cells.

Immunofluorescence Localization

We then examined the localization of β_4 within the conventional outflow pathway of C57BL/6J mice using confocal immunofluorescence (Fig. 1). β_4 was observed in the TM, labeling subendothelial cells underlying the inner and outer walls of SC. Continuous bands of β_4 labeling were observed in the internal TM, suggestive of labeling along trabecular beams. Punctate labeling of β_4 was observed along the inner and outer walls of SC, identified by CD31. The punctate β_4 labeling along SC endothelium often appeared as extensions of β_4 labeling within the subendothelial space, suggestive of junctional processes connecting subendothelial or juxtacanalicular cells to the basal surface of SC endothelium.^{32–34} β_4 labeling was also observed along ciliary process capillaries, the ciliary epithelium, and in nerve bundles within the sclera and cornea. Moderate β_4 labeling was observed in the ciliary muscle.

Outflow Facility

We then examined the effect of two $K_{Ca}1.1$ blockers, IbTX and MarTX, on outflow facility in enucleated mouse eyes using the iPerfusion system.³⁰ IbTX predominately blocks $K_{Ca}1.1$ channels that contain only α -subunits or $\alpha+\beta_1$ subunits, but IbTX does not effectively block $K_{Ca}1.1$ that contain β_4 .¹⁸ In response to 100 or 500 nM IbTX, outflow facility decreased by 16% [6%, 25%] (geometric mean, [95% confidence interval]) relative to contralateral eyes that were perfused with vehicle ($P = 0.01$, $n = 9$ pairs; paired two-tailed t -test; Figs. 2A, 2B). Data for both concentrations were pooled together because there was no statistical difference between 100 and 500 nM IbTX ($P = 0.6$; $n = 4$ and 5) for the present data (unpaired two-tailed t -test). C_r for IbTX-treated eyes was 5.0 [3.8, 6.2] nL/min/mm Hg versus 5.9 [4.8, 7.1] nL/min/mm Hg for vehicle-treated eyes.

MarTX is a potent and selective blocker of β_4 -containing $K_{Ca}1.1$ channels.¹⁹ In response to 100 nM MarTX, outflow facility decreased by 35% [27%, 42%] ($P < 0.0001$, $n = 12$; Figs. 2C, 2D) relative to vehicle-treated contralateral eyes. C_r for MarTX-treated eyes was 4.3 [3.2, 5.5] nL/min/mm Hg compared with 6.7 [5.5, 8.0] nL/min/mm Hg for vehicle-treated eyes. The effect of MarTX on C_r was significantly greater than that of IbTX ($P = 0.01$, unpaired two-tailed t -test).

To examine whether MarTX induces cellular toxicity in the outflow pathway, we used transmission electron microscopy to visualize the ultrastructure of the TM in a pair of eyes perfused with MarTX or vehicle. There were no obvious morphological differences between MarTX and vehicle-perfused eyes. In both cases, the inner wall of SC appeared continuous, and the juxtacanalicular connective tissue (JCT) contained loose extracellular matrix interspersed by JCT cells that extended connections to the inner wall and TM beams (Figs. 3A, 3C). The mitochondria appeared normal without any evidence of swelling that would indicate toxicity, and cell membranes and cell-cell connections appeared intact (Figs. 3B, 3D). This suggests that MarTX does not induce an overtly toxic effect in the outflow pathway.

DISCUSSION

The large-conductance calcium-activated potassium channel $K_{Ca}1.1$ is a known regulator of outflow facility. Opening $K_{Ca}1.1$ with NS1619 increases outflow facility in porcine anterior segments.¹³ Conversely, blocking $K_{Ca}1.1$ with IbTX prevents the increase in outflow facility following treatment with nitric oxide¹⁵ or perfusion with hypotonic saline.⁵ Here we show that blocking $K_{Ca}1.1$, with either IbTX or MarTX, independent of nitric oxide or any other stimulus, decreases outflow facility in enucleated mouse eyes. Thus across different species, opening the $K_{Ca}1.1$ channel coincides with increasing outflow facility, whereas blockade of the $K_{Ca}1.1$ channel corresponds with decreasing outflow facility.

$K_{Ca}1.1$ may modulate outflow facility by influencing cell contractility. Opening $K_{Ca}1.1$ leads to potassium efflux and membrane hyperpolarization that inactivates voltage-gated calcium channels.¹⁶ The associated reduction in cytosolic

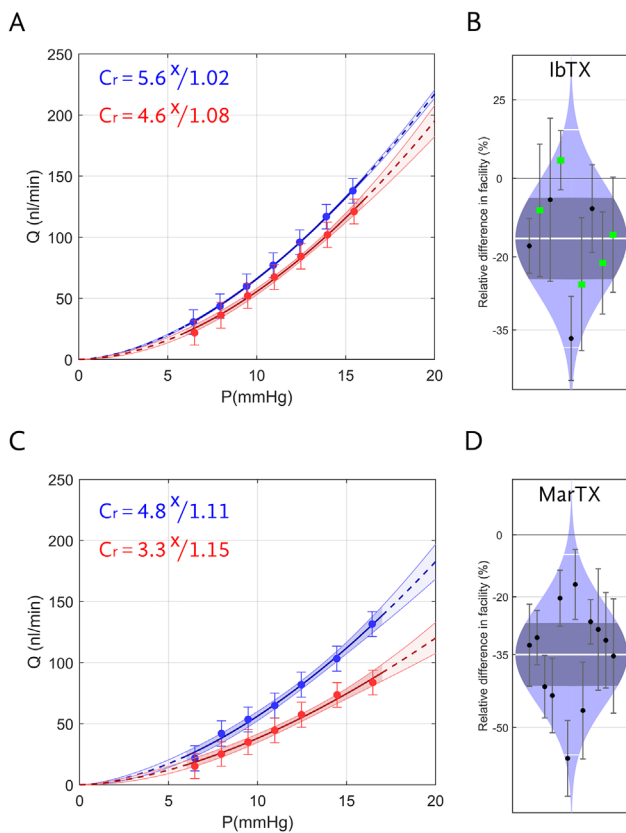


FIGURE 2. Representative flow-pressure (Q-P) plots of eyes treated with IbTX (A) or MarTX (C) versus vehicle-perfused contralateral eyes. *Error bars* are 95% confidence intervals. Relative difference in facility for IbTX (B) and MarTX (D) treated eyes. The relative difference in facility is defined as the ratio of C_r in the treated eye relative to that in the untreated contralateral eye minus unity, expressed as a percentage. Each data point represents the relative difference in facility for an individual mouse. *Error bars* are 95% confidence intervals. Shaded regions represent the best estimate of the sample distributions, with the central *white line* representing the geometric mean. Dark central bands represent the 95% confidence interval on the mean, and the outer *white lines* represent the limits encompassing 95% of the population. *Green squares* in (B) correspond to data obtained from 500 nM IbTX and *black circles* from 100 nM. The C_r values appearing in (A, C) correspond to the Q-P data shown in each plot, in units of nL/min/mm Hg.

calcium leads to relaxation in smooth muscle cells.⁹ Similarly, opening $K_{Ca}1.1$ leads to relaxation in TM and ciliary muscle cells and a reduction in calcium-induced actin polymerization.^{7,35} Cell relaxation is typically associated with increasing outflow facility, as occurs following treatment with rho kinase inhibitors^{36,37} or nitric oxide.^{38,39}

Alternatively, $K_{Ca}1.1$ channel opening may lead to water efflux across the cell membrane and a reduction in TM and SC cell volume.^{5,6} Because aqueous humor passes through narrow tortuous spaces in the juxtacanalicular TM and through micron-sized pores in the inner wall endothelium of SC, relatively small changes in cell volume at flow-limiting sites can have significant effects on outflow facility. Consistent with this notion, the increase in outflow facility following perfusion with hypertonic saline coincides with a widening of open spaces in the juxtacanalicular TM.⁴⁰ Similarly, treatment with nitric oxide decreases cell volume in TM and SC cells in vitro, and the time scale for cell

volume change corresponds to the time scale for changing outflow facility.^{6,15} Blocking $K_{Ca}1.1$ with IbTX inhibits both the effect of nitric oxide on TM and SC cell volume and on outflow facility.^{6,13,15} Thus $K_{Ca}1.1$ channel opening appears to increase outflow facility by promoting cellular volume reduction and/or cell relaxation in the outflow pathway. Conversely, blocking $K_{Ca}1.1$ with IbTX or MarTX should decrease outflow facility by inhibiting relaxation and/or cell volume decrease. In addition, because cell volume regulation is tightly coupled to mechanical stretch and contractility experienced by TM cells,⁴¹ it may not be possible to attribute the effects of $K_{Ca}1.1$ to cell volume or contractility alone.

Other potassium ion channels, in addition to $K_{Ca}1.1$, have similar effects on outflow facility. Opening the ATP-sensitive inward rectifier potassium channel 11 ($K_{ir}6.2$) with cromakalim,⁴² or its prodrug CKLP1,⁴³ increases outflow facility in human anterior segments and reduces IOP in wild-type mice, but not in homozygous null mice lacking $K_{ir}6.2$.⁴² Despite the IOP-lowering effect of cromakalim/CKLP1, there was no detectable effect of CKLP1 on pressure-dependent outflow facility in either enucleated or in vivo mice,⁴³ leading the authors to conclude that K_{ir} opening by CKLP1 may affect distal outflow.

Activity of $K_{Ca}1.1$ is regulated by auxiliary β -subunits that affect channel sensitivity to intracellular calcium and membrane voltage.^{16,17} Of the four known β -subunits, we show that β_4 is the most highly expressed in the anterior segment of the mouse eye. In cultured human SC cells, we show that β_4 appears to be the sole β -subunit, and β_4 is the primary β -subunit expressed by human TM cells. The β -subunit expression profile influences the pharmacology of the $K_{Ca}1.1$ channel. IbTX and MarTX, for example, are venomous scorpion toxins that are evolutionarily selected to be highly specific for particular β -subunit combinations of $K_{Ca}1.1$. IbTX completely blocks ion channels composed solely of pore-forming α -subunits that are present in all $K_{Ca}1.1$ channels, but IbTX only partially blocks β_1 -containing $K_{Ca}1.1$ channels (by $\sim 50\%$) and ineffectively blocks β_4 -containing $K_{Ca}1.1$ channels (by $\sim 20\%$).¹⁸ MarTX, in contrast, is highly selective for β_4 -containing $K_{Ca}1.1$ channels, with an IC₅₀ value of 21 to 78 nM,^{19,28} and MarTX has a negligible effect on $K_{Ca}1.1$ channels containing only α -subunits.¹⁹ MarTX also has a negligible effect on β_1 -containing $K_{Ca}1.1$ channels for concentrations up to 400 nM with low cytoplasmic calcium.⁴⁴ However, with high cytoplasmic calcium, MarTX enhances β_1 -containing $K_{Ca}1.1$ channel activity with an EC₅₀ of 495 nM.⁴⁵ Taken together, the 100 nM concentration of MarTX used in this study should have had little effect on β_1 -containing $K_{Ca}1.1$ channels, as β_1 was the second most highly expressed β -subunit after β_4 in TM cells and in mouse anterior segments.

In response to IbTX, we measured a significant decrease in outflow facility in enucleated mouse eyes. This suggests that at least some of the channels involved in facility regulation are IbTX-sensitive (i.e., β_4 -deficient), consistent with prior reports.^{5,6} However, MarTX, which selectively blocks β_4 -containing $K_{Ca}1.1$ channels, had a nearly two-fold larger facility reduction relative to IbTX ($\sim 35\%$ vs. $\sim 16\%$ average reduction). Although the MarTX and IbTX experiments were performed in separate cohorts such that the data are not directly comparable, the larger facility effect observed with MarTX suggests that the majority of $K_{Ca}1.1$ channels involved in outflow facility regulation contain the β_4 -subunit. However, further study would be necessary to confirm within the same cohort whether MarTX

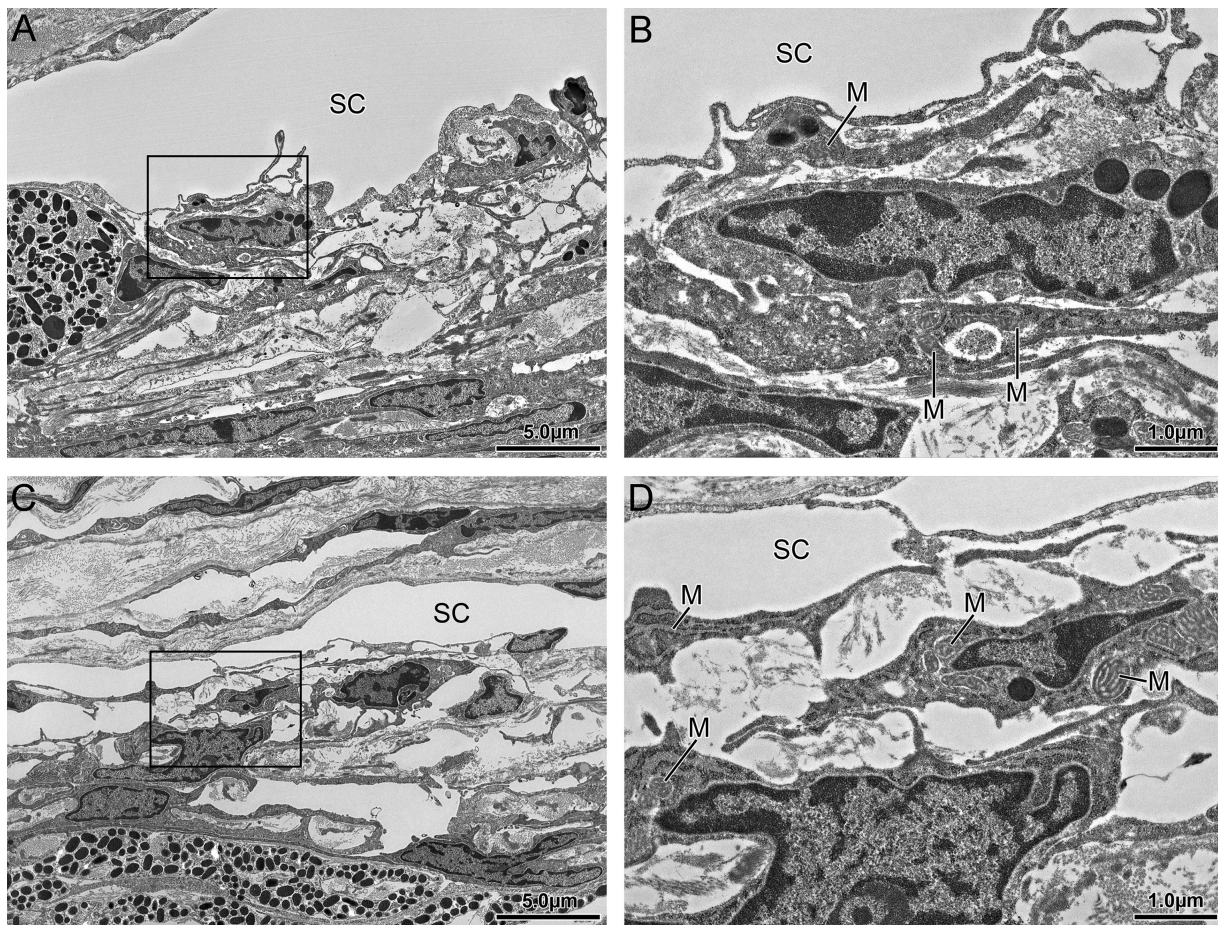


FIGURE 3. Sagittal sections of paired mouse eyes perfused with vehicle (**A, B**) or 100 nM MarTX (**C, D**) imaged by transmission electron microscopy. Boxed regions in (**A, C**) are shown magnified in (**B, D**). M, mitochondria. Scale bars are 5 μ m in (**A, C**) and 1 μ m in (**B, D**).

truly has additive inhibitory effects beyond IbTX. Regardless, the magnitude of the facility reduction measured in response to MarTX was comparable to that previously reported in response to sphingosine 1-phosphate,⁴⁶ reduced temperature,⁴⁷ and prolonged exposure to dexamethasone.⁴⁸ Thus β_4 -containing $K_{Ca}1.1$ channels appear to be centrally important for the maintenance of outflow because blocking these channels significantly disrupts outflow function.

Using confocal microscopy, we localized expression of β_4 to the juxtacanalicular TM, with punctate labeling observed along the endothelium of SC. This labeling pattern was consistent with β_4 expression along cell processes that connect juxtacanalicular TM cells with inner wall cells.^{32,33,48–50} These processes experience significant biomechanical deformation in response to IOP elevation.^{34,51–53} As the juxtacanalicular TM and inner wall of SC are the primary sites of outflow resistance generation,^{1,2} this localization suggests a mechanosensory and regulatory role for β_4 . Specifically, we postulate the existence of a stretch-sensitive feedback loop whereby β_4 -containing $K_{Ca}1.1$ channels are opened in response to IOP-induced stretch in the juxtacanalicular TM, triggering signaling pathways that lead to increased outflow facility to oppose the elevation in IOP. Previous studies have provided evidence that $K_{Ca}1.1$ channels in bovine TM are directly sensitive to stretch, independent of cytosolic calcium levels.¹² Even if $K_{Ca}1.1$ channels are not directly stretch-activated, $K_{Ca}1.1$ may be acti-

vated by elevated intracellular calcium that often occurs in response to stretch or other mechanical stimulation. Consequently, we hypothesize that the association with particular β -subunits influence the mechanosensitivity of $K_{Ca}1.1$ in the juxtacanalicular TM. For example, the β_4 -subunit regulates shear and stretch-mediated mechanotransduction in intercalated cells of the kidney collecting duct.^{54,55} Similarly, β_4 may influence mechanotransduction via $K_{Ca}1.1$ in the juxtacanalicular TM.

Stretch induces secretion of several compounds from TM cells that increase outflow facility, such as adenosine triphosphate,⁵⁶ metalloproteinases,⁵⁷ and vascular endothelial growth factor.⁵⁸ As $K_{Ca}1.1$ appears to be involved in the stretch response in TM cells, it is possible that blocking $K_{Ca}1.1$ may suppress stretch-induced release of these compounds to oppose the facility increase. $K_{Ca}1.1$ is also involved in homeostatic regulation of cell volume, as occurs during the regulatory volume decrease following hypoosmotic shock. As regulatory volume decrease is associated with increasing outflow facility,⁵⁹ blocking $K_{Ca}1.1$ could potentially affect cell volume regulation in the TM to affect outflow facility.

CONCLUSIONS

We have shown that β_4 is the primary β -subunit of $K_{Ca}1.1$ expressed in outflow pathway tissues. Blockade of β_4 -

containing K_{Ca} 1.1 channels with MarTX leads to a physiologically significant decrease in outflow facility, which appeared to be larger than observed when blocking K_{Ca} 1.1 channels that lack β_4 with IbTX. The β_4 -subunit is localized to the juxtacanalicular TM and inner wall of SC, where it may influence the response of these tissues to IOP-induced stretch or shear stress. The β_4 -subunit is thus important for outflow regulation, potentially by influencing mechanotransduction via K_{Ca} 1.1. Compounds that modulate β_4 - K_{Ca} 1.1 activity should therefore be explored as an approach to improve outflow and lower IOP for glaucoma therapy.

Acknowledgments

The authors thank Kristin Perkumas (Duke University) for isolation and characterization of human trabecular meshwork and Schlemm's canal cells.

Supported by Fight for Sight (UK; Grant 1858), the National Institutes of Health (EY022359), and the National Multiple Sclerosis Society—Fast Forward group (FF-1602-07939).

Prior publications: 2019 ARVO abstract, Blockade of the BK_{α/β_4} potassium ion channel reduces outflow facility in mice.

Disclosure: **J.A. Bertrand**, None; **M. Schicht**, None; **W.D. Stamer**, None; **D. Baker**, None; **J.M. Sherwood**, None; **E. Lütjen-Drecoll**, None; **D.L. Selwood**, None; **D.R. Overby**, None

References

- Lütjen-Drecoll E. Structural factors influencing outflow facility and its changeability under drugs. A study in *Macaca arctoides*. *Invest Ophthalmol*. 1973;12:280–294.
- Mäepea O, Bill A. Pressures in the juxtacanalicular tissue and Schlemm's canal in monkeys. *Exp Eye Res*. 1992;54:879–883.
- Overby DR, Stamer WD, Johnson M. The changing paradigm of outflow resistance generation: towards synergistic models of the JCT and inner wall endothelium. *Exp Eye Res*. 2009;88:656–670.
- Raghunathan VK, Benoit J, Kasetti R, et al. Glaucomatous cell derived matrices differentially modulate non-glaucomatous trabecular meshwork cellular behavior. *Acta Biomater*. 2018;71:444–459.
- Soto D, Comes N, Ferrer E, et al. Modulation of aqueous humor outflow by ionic mechanisms involved in trabecular meshwork cell volume regulation. *Invest Ophthalmology Vis Sci*. 2004;45:3650.
- Ellis DZ, Sharif NA, Dismuke WM. Endogenous regulation of human Schlemm's canal cell volume by nitric oxide signaling. *Invest Ophthalmol Vis Sci*. 2010;51:5817–5824.
- Wiederholt M, Thieme H, Stumpff F. The regulation of trabecular meshwork and ciliary muscle contractility. *Prog Retin Eye Res*. 2000;19:271–295.
- Overby DR, Zhou EH, Vargas-Pinto R, et al. Altered mechanobiology of Schlemm's canal endothelial cells in glaucoma. *Proc Natl Acad Sci USA*. 2014;111:13876–13881.
- Contreras GF, Castillo K, Enrique N, et al. A BK (Slo1) channel journey from molecule to physiology. *Channels (Austin)*. 2013;7:442–458.
- Stumpff F, Strauss O, Boxberger M, Wiederholt M. Characterization of maxi-K-channels in bovine trabecular meshwork and their activation by cyclic guanosine monophosphate. *Invest Ophthalmol Vis Sci*. 1997;38:1883–1892.
- Stumpff F, Que Y, Boxberger M, Strauss O, Wiederholt M. Stimulation of maxi-K channels in trabecular meshwork by tyrosine kinase inhibitors. *Invest Ophthalmol Vis Sci*. 1999;40:1404–1417.
- Gasull X, Ferrer E, Llobet A, et al. Cell membrane stretch modulates the high-conductance Ca^{2+} -activated K^{+} channel in bovine trabecular meshwork cells. *Invest Ophthalmol Vis Sci*. 2003;44:706–714.
- Dismuke WM, Ellis DZ. Activation of the BK_{Ca} channel increases outflow facility and decreases trabecular meshwork cell volume. *J Ocul Pharmacol Ther*. 2009;25:309–314.
- Holland M, Langton PD, Standen NB, Boyle JP. Effects of the BK_{Ca} channel activator, NS1619, on rat cerebral artery smooth muscle. *Br J Pharmacol*. 1996;117:119–129.
- Dismuke WM, Mbadugha CC, Ellis DZ. NO-induced regulation of human trabecular meshwork cell volume and aqueous humor outflow facility involve the BK_{Ca} ion channel. *Am J Physiol Cell Physiol*. 2008;294:C1378–C1386.
- Kaczmarek LK, Aldrich RW, Chandy KG, Grissmer S, Wei AD, Wulff H. International union of basic and clinical pharmacology. C. Nomenclature and properties of calcium-activated and sodium-activated potassium channels. *Pharmacol Rev*. 2017;69:1–11.
- Contreras GF, Neely A, Alvarez O, Gonzalez C, Latorre R. Modulation of BK channel voltage gating by different auxiliary subunits. *Proc Natl Acad Sci USA*. 2012;109:18991–18996.
- Meera P, Wallner M, Toro L. A neuronal beta subunit (KCNMB4) makes the large conductance, voltage- and Ca^{2+} -activated K^{+} channel resistant to charybdotoxin and iberiotoxin. *Proc Natl Acad Sci USA*. 2000;97:5562–5567.
- Shi J, He HQ, Zhao R, et al. Inhibition of martenoxin on neuronal BK channel subtype ($\alpha + \beta_4$): implications for a novel interaction model. *Biophys J*. 2008;94:3706–3713.
- Tao J, Zhou ZL, Wu B, Shi J, Chen XM, Ji YH. Recombinant expression and functional characterization of martenoxin: a selective inhibitor for BK channel ($\alpha + \beta_4$). *Toxins (Basel)*. 2014;6:1419–1433.
- Thompson CL, Ng L, Menon V, et al. A high-resolution spatiotemporal atlas of gene expression of the developing mouse brain. *Neuron*. 2014;83:309–323.
- Zhang X-H, Zhang Y-Y, Sun H-Y, Jin M-W, Li G-R. Functional ion channels and cell proliferation in 3T3-L1 preadipocytes. *J Cell Physiol*. 2012;227:1972–1979.
- Stamer WD, Seftor RE, Williams SK, Samaha HA, Snyder RW. Isolation and culture of human trabecular meshwork cells by extracellular matrix digestion. *Curr Eye Res*. 1995;14:611–617.
- Stamer WD, Roberts BC, Howell DN, Epstein DL. Isolation, culture, and characterization of endothelial cells from Schlemm's canal. *Invest Ophthalmol Vis Sci*. 1998;39:1804–1812.
- Perkumas KM, Stamer WD. Protein markers and differentiation in culture for Schlemm's canal endothelial cells. *Exp Eye Res*. 2012;96:82–87.
- Keller KE, Bhattacharya SK, Borrás T, et al. Consensus recommendations for trabecular meshwork cell isolation, characterization and culture. *Exp Eye Res*. 2018;171:164–173.
- Baker D, Pryce G, Visintin C, et al. Big conductance calcium-activated potassium channel openers control spasticity without sedation. *Br J Pharmacol*. 2017;174:2662–2681.
- Ji Y-H, Wang W-X, Ye J-G, et al. Martentoxin, a novel K^{+} -channel-blocking peptide: purification, cDNA and genomic cloning, and electrophysiological and pharmacological characterization. *J Neurochem*. 2003;84:325–335.
- Wang Y, Chen X, Zhang N, Wu G, Wu H. The solution structure of $BmTx3B$, a member of the scorpion toxin subfamily alpha-KTx 16. *Proteins*. 2005;58:489–497.

30. Sherwood JM, Reina-Torres E, Bertrand JA, Rowe B, Overby DR. Measurement of outflow facility using iPerfusion. *PLoS One*. 2016;11:e0150694.
31. Porter KM, Epstein DL, Liton PB. Up-regulated expression of extracellular matrix remodeling genes in phagocytically challenged trabecular meshwork cells. *PLoS One*. 2012;7:7–9.
32. Lütjen-Drecoll E, Rohen JW. Functional morphology of the trabecular meshwork. In: Tasman W, ed. *Duane's Foundation of Clinical Ophthalmology*. Philadelphia, PA: J.B. Lippincott; 1992:1–33.
33. Epstein DL, Rohen JW. Morphology of the trabecular meshwork and inner-wall endothelium after cationized ferritin perfusion in the monkey eye. *Invest Ophthalmol Vis Sci*. 1991;32:160–171.
34. Grierson I, Lee WR. Pressure effects on flow channels in the lining endothelium of Schlemm's canal. A quantitative study by transmission electron microscopy. *Acta Ophthalmol*. 1978;56:935–952.
35. Stumpff F, Wiederholt M. Regulation of trabecular meshwork contractility. *Ophthalmol J Int d'ophtalmologie Int J Ophthalmol Zeitschrift fur Augenheilkd*. 2000;214:33–53.
36. Honjo M, Tanihara H, Inatani M, et al. Effects of rho-associated protein kinase inhibitor Y-27632 on intraocular pressure and outflow facility. *Invest Ophthalmol Vis Sci*. 2001;42:137–144.
37. Li G, Mukherjee D, Navarro I, et al. Visualization of conventional outflow tissue responses to netarsudil in living mouse eyes. *Eur J Pharmacol*. 2016;787:20–31.
38. Schuman JS, Erickson K, Nathanson JA. Nitrovasodilator effects on intraocular pressure and outflow facility in monkeys. *Exp Eye Res*. 1994;58:99–105.
39. Chang JYH, Stamer WD, Bertrand J, et al. Role of nitric oxide in murine conventional outflow physiology. *Am J Physiol Cell Physiol*. 2015;309:C205–C214.
40. Al-Aswad LA, Gong H, Lee D, et al. Effects of Na-K-2Cl cotransport regulators on outflow facility in calf and human eyes in vitro. *Invest Ophthalmol Vis Sci*. 1999;40:1695–1701.
41. Baetz NW, Hoffman EA, Yool AJ, Stamer WD. Role of aquaporin-1 in trabecular meshwork cell homeostasis during mechanical strain. *Exp Eye Res*. 2009;89:95–100.
42. Chowdhury UR, Bahler CK, Holman BH, Dosa PI, Fautsch MP. Ocular hypotensive effects of the ATP-sensitive potassium channel opener cromakalim in human and murine experimental model systems. *PLoS One*. 2015;10:e0141783.
43. Chowdhury UR, Rinkoski TA, Bahler CK, et al. Effect of cromakalim prodrug 1 (CKLP1) on aqueous humor dynamics and feasibility of combination therapy with existing ocular hypotensive agents. *Invest Ophthalmol Vis Sci*. 2017;58:5731–5742.
44. Tao J, Shi J, Liu Z-R, Ji Y-H. Martentoxin: a unique ligand of BK channels. *Sheng Li Xue Bao*. 2012;64:355–364.
45. Tao J, Shi J, Yan L, et al. Enhancement effects of martentoxin on glioma BK channel and BK channel ($\alpha+\beta$ 1) subtypes. *PLoS One*. 2011;6:e15896.
46. Boussommier-Calleja A, Bertrand J, Woodward DF, Ethier CR, Stamer WD, Overby DR. Pharmacologic manipulation of conventional outflow facility in ex vivo mouse eyes. *Invest Ophthalmol Vis Sci*. 2012;53:5838–5845.
47. Boussommier-Calleja A, Li G, Wilson A, et al. Physical factors affecting outflow facility measurements in mice. *Invest Ophthalmol Vis Sci*. 2015;56:8331–8339.
48. Overby DR, Bertrand J, Tektas OY, et al. Ultrastructural changes associated with dexamethasone-induced ocular hypertension in mice. *Invest Ophthalmol Vis Sci*. 2014;55:4922–4933.
49. Grierson I, Lee WR, Abraham S, Howes RC. Associations between the cells of the walls of Schlemm's canal. *Albrecht Von Graefes Arch Klin Exp Ophthalmol*. 1978;208:33–47.
50. Gong H, Tripathi RC, Tripathi BJ. Morphology of the aqueous outflow pathway. *Microsc Res Tech*. 1996;33:336–367.
51. Johnstone MA. Pressure-dependent changes in nuclei and the process origins of the endothelial cells lining Schlemm's canal. *Invest Ophthalmol Vis Sci*. 1979;18:44–51.
52. Ye W, Gong H, Sit A, Johnson M, Freddo TF. Interendothelial junctions in normal human Schlemm's canal respond to changes in pressure. *Invest Ophthalmol Vis Sci*. 1997;38:2460–2468.
53. Sherwood JM, Stamer WD, Overby DR. A model of the oscillatory mechanical forces in the conventional outflow pathway. *J R Soc Interface*. 2019;16:20180652.
54. Holtzclaw JD, Liu L, Grimm PR, Sansom SC. Shear stress-induced volume decrease in C11-MDCK cells by BK- α/β 4. *Am J Physiol Renal Physiol*. 2010;299:F507–F516.
55. Pacha J, Frindt G, Sackin H, Palmer LG. Apical maxi-K channels in intercalated cells of Cct. *Am J Physiol*. 1991;261:F696–F705.
56. Luna C, Li G, Qiu J, Challa P, Epstein DL, Gonzalez P. Extracellular release of ATP mediated by cyclic mechanical stress leads to mobilization of AA in trabecular meshwork cells. *Invest Ophthalmol Vis Sci*. 2009;50:5805–5810.
57. Bradley JMB, Kelley MJ, Zhu X, Anderssohn AM, Alexander JP, Acott TS. Effects of mechanical stretching on trabecular matrix metalloproteinases. *Invest Ophthalmol Vis Sci*. 2001;42:1505–1513.
58. Reina-Torres E, Wen JC, Liu KC, et al. VEGF as a paracrine regulator of conventional outflow facility. *Invest Ophthalmol Vis Sci*. 2017;58:1899–1908.
59. Li A, Leung CT, Peterson-Yantorno K, Stamer WD, Civan MM. Cytoskeletal dependence of adenosine triphosphate release by human trabecular meshwork cells. *Invest Ophthalmol Vis Sci*. 2011;52:7996–8005.